

# Design of Tri-Substituted Dodecatungstosilicate from a Trilacunary Silicotungstate by Insertion of Manganese Ions of $[\text{Mn}_3(\mu_3\text{-O})(2\text{-Cl-benzoato})_6(\text{py})_3]$ : Synthesis, Structure, Redox and Magnetic Studies

Daipayan Dutta,<sup>[a]</sup> Atish D. Jana,<sup>[b]</sup> Mainak Debnath,<sup>[a]</sup> Golam Mostafa,<sup>[b]</sup>  
Rodolphe Clérac,<sup>[c,d]</sup> Javier G. Tojal,<sup>[e]</sup> and Mohammad Ali\*<sup>[a]</sup>

**Keywords:** Polyoxometalates / Silicates / Manganese / Mixed-valent compounds / Magnetic properties

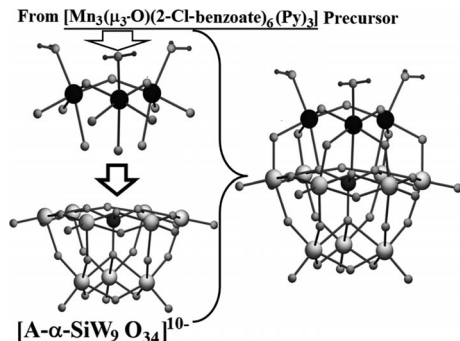
A mixed-valent manganese tricapped Keggin polyoxometalate (**3**) has been designed by insertion of three Mn atoms from  $[\text{Mn}^{\text{II}}\text{Mn}^{\text{III}}_2(\mu_3\text{-O})(2\text{-Cl-benzoato})_6(\text{py})_3]$  (**1**) into the vacant sites of the trilacunary precursor  $\text{Na}_{10}[\text{A-}\alpha\text{-SiW}_9\text{O}_{34}]$  (**2**). This compound exhibits strong antiferromagnetic interaction between the spin carriers of the Mn mixed-valent trinuclear moiety, which suggests an  $S = 5/2$  ground state.

Considering the importance of these tri-substituted Keggin POMs as a model for soluble catalytic metal oxide surfaces<sup>[9]</sup> and the possibility of tuning the spin-exchange behaviour within the substituted transition-metal complexes<sup>[10]</sup> we felt the need to find rational synthetic procedures to obtain tri-substituted POMs with mixed-valent metal environments. Therefore, a novel strategy was adopted by considering a suitable manganese precursor containing a trinuclear mixed-valent  $[\text{Mn}^{\text{II}}\text{Mn}^{\text{III}}_2]$  complex,  $[\text{Mn}_3(\mu_3\text{-O})(2\text{-Cl-benzoato})_6(\text{py})_3]$  (**1**, with py = pyridine),<sup>[11]</sup> that could eventually occupy the three vacant sites of the lacunary silicotungstate precursor  $\text{Na}_{10}[\text{A-}\alpha\text{-SiW}_9\text{O}_{34}]$  (**2**) and ultimately build up the transition-metal substituted Keggin polyanion (**3**) (Scheme 1).

## Introduction

Polyoxometalates (hereafter designated as POMs) constitute an important class of materials that exhibit versatile electronic properties as well as structural diversity. This leads to applications in numerous fields such as catalysis,<sup>[1]</sup> material science and magnetism,<sup>[2]</sup> medicine,<sup>[3]</sup> photochemistry,<sup>[4]</sup> bio- and nanotechnology<sup>[5]</sup> etc. While the mechanism of POM formation remains a poorly understood phenomenon, researchers often utilize natural self-assembly processes to functionalize POMs by choosing suitable building blocks and by exploring proper reaction conditions. Indeed, the rational synthesis of POMs is still a dream goal of synthetic chemists in this field of research, but the knowledge gained so far indicates that sandwich-type complexes are the usual final products when transition-metal ions react with dilacunary POM precursors,<sup>[6]</sup> and, in most of the cases, the structure of the POM precursor is preserved. Although, dilacunary tungstosilicates have been used extensively by different groups,<sup>[2,6,7]</sup> the use of trilacunary tungstosilicates for surface modification of POMs is limited.<sup>[8]</sup> Pope and co-workers<sup>[9]</sup> synthesized a series of trimetallo derivatives  $\text{SiW}_9\text{M}_3$  of both  $\alpha$ - and  $\beta$ -isomers with  $\text{M} = \text{Cr}^{\text{III}}, \text{Fe}^{\text{III}}, \text{Mn}^{\text{II}}, \text{Co}^{\text{II}}, \text{Ni}^{\text{II}}$  and  $\text{Cu}^{\text{II}}$ , but failed to get X-ray quality single crystals, and hence the magnetic properties were not analyzed in relation with the structural information.

From  $[\text{Mn}_3(\mu_3\text{-O})(2\text{-Cl-benzoato})_6(\text{Py})_3]$  Precursor



$[\text{A-}\alpha\text{-SiW}_9\text{O}_{34}]^{10-}$

Scheme 1.

## Results and Discussion

### Syntheses and Structural Characterization

The mixed-valent tri-manganese-substituted Keggin-type dodecatungstosilicate (**3**) was synthesized by a simple one-

[a] Department of Chemistry, Jadavpur University, Kolkata 700032, India  
E-mail: m\_ali2062@yahoo.com

[b] Department of Physics, Jadavpur University, Kolkata 700032, India

[c] CNRS, UPR 8641, Centre de Recherche Paul Pascal (CRPP), Equipe "Matériaux Moléculaires Magnétiques", 115 avenue du Dr. Albert Schweitzer, 33600 Pessac, France

[d] Université de Bordeaux, UPR 8641, 33600 Pessac, France

[e] Departamento de Química, Universidad de Burgos, Plaza Misael Bañuelos s/n, 09001 Burgos, Spain

pot reaction of tri-lacunary 9-tungstosilicate (**2**) with  $[\text{Mn}^{\text{II}}\text{Mn}^{\text{III}}_2(\mu_3\text{-O})(2\text{-Cl-benzoato})_6(\text{py})_3]$  (**1**) in aqueous acetic acid medium (pH = 4.50). The composition of **3** is supported by elemental analysis and a TGA study, which shows a loss of weight of ca. 7.10% that corresponds to a loss of 24 water molecules (7.35%) from its unit-cell volume. At room temperature, complex **3** is fairly stable in air and also soluble in water.

The X-ray crystallographic analysis reveals that tri-lacunary  $[\text{A-}\alpha\text{-SiW}_9\text{O}_{34}]^{10-}$  (**2**) takes up three manganese ions from **1** to give a highly symmetrical polyanion **3** (Figure 1). The central tetrahedral Si site is surrounded by twelve octahedra, of which nine have W and three have Mn at their centres (Figure 2). The O atoms are located at the vertices of each of the polyhedra. Four O atoms (O1, O5, O5\*, O5\*\*, \*:  $1 - y, x - y, z$ ; \*\*:  $1 - x + y, 1 - x, z$ ) connected to tetrahedral Si (Si4) constitute the common vertex of three edge-shared octahedra, which divide the twelve octahedra into 4 groups. Three of these groups are identical, in which two W octahedra and one Mn octahedron share common edges; in the other group, the edges are shared by three W octahedra (Figure 2). The anion is highly symmetric with a  $C_3$  symmetry. It is worth mentioning that the

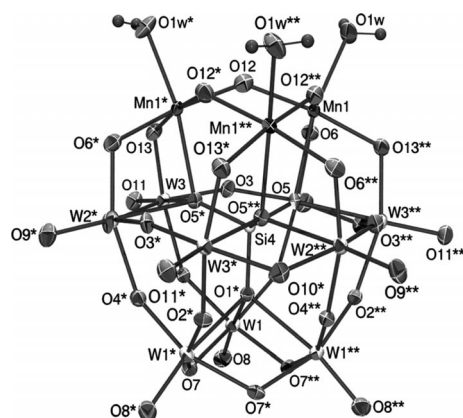


Figure 1. ORTEP diagram with atom numbering scheme of the  $[\text{Mn}^{\text{II}}\text{Mn}^{\text{III}}_2(\text{H}_2\text{O})_3\text{SiW}_9\text{O}_{37}]^{8-}$  ion (**3**) (30% ellipsoidal probability). Symmetry operators \*:  $1 - y, x - y, z$  and \*\*:  $1 - x + y, 1 - x, z$ .

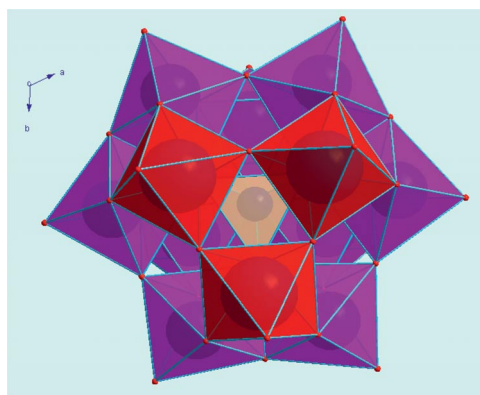


Figure 2. Polyhedral presentation of  $[\text{Mn}^{\text{II}}\text{Mn}^{\text{III}}_2(\text{H}_2\text{O})_3\text{SiW}_9\text{O}_{37}]^{8-}$  anion (**3**). The  $\text{SiO}_4$ ,  $\text{WO}_6$ ,  $\text{MnO}_6$  polyhedra are shown in brown, violet and red, respectively.

manganese precursor that was used to occupy the lacunary sites of the parent polyoxoanion, also exhibits a  $C_3$  symmetry. A recent report on grafting a  $\text{Mn}_6\text{Ce}$ -carboxylate complex on the vacant sites of a tri-lacunary Wells–Dawson-type POM gives another example of our synthetic approach.<sup>[12]</sup> Interestingly, the  $\text{Mn}_6\text{Ce}$ -carboxylate precursor retains its molecular core after grafting onto the POM surface, even if the symmetry of the vacant sites on the POM surface do not match those of the precursor. This self-assembly was possible, likely because the reaction was carried out in strong acetic acid medium that prevents the removal of coordinated carboxylate ions. In the present case, the Keggin POM has a  $C_3$ -symmetric vacant site as well as a guest precursor in order to fit suitably into the cavity. The removal of benzoate groups occurs as a result of the fact that the reaction was carried out in aqueous MeCN buffered with dilute NaOAc/AcOH at pH = 4.50, and under such conditions, the surface oxygen atoms are assumed to be sufficiently basic to displace the benzoate groups.

Mn–O bond lengths along the joining lines of the three Mn centres that form the cap of the POM are alternately 1.978(9) Å (Mn1–O12) and 2.006(9) Å (Mn1–O12\*\*). The Mn centres form an equilateral triangular arrangement of Mn atoms and the  $C_3$  axis passes through its centre. The terminal oxygen atoms (O1W, O1W\*, O1W\*\*) attached to three Mn centres are water molecules with an Mn–O distance of 2.160(8) Å; the other oxygen atoms act as oxo bridges.

Bond valence sum (BVS) values<sup>[13]</sup> for the oxygen atoms in the polyanion fall in the range 1.59–2.03, with the exception of Mn–O1W with a BVS value of 0.33. The former oxygen atoms (W–O/Mn–O) are presumed to arise from oxo groups, while the later (attached to Mn) are terminal oxygen atoms from water molecules and this result is consistent with other manganese(III)-substituted polyanions with terminal aqua ligands.<sup>[14]</sup> The BVS of tungsten (5.97–6.22) and silicon (3.96) fall within the expected limits. The BVS of three manganese atoms (2.76) indicates a mixed-valence  $[\text{Mn}_3]$  unit with one  $\text{Mn}^{\text{II}}$  and two  $\text{Mn}^{\text{III}}$  atoms; this result is also consistent with those obtained from the magnetic data (vide infra). It is difficult to differentiate crystallographically the  $\text{Mn}^{\text{II}}$  and  $\text{Mn}^{\text{III}}$  sites, as the three Mn atoms are threefold-symmetry related and are equivalent. According to the BVS value and magnetic data, a disordered model is proposed for the Mn sites in which every Mn position is occupied by  $\text{Mn}^{\text{II}}$  and  $\text{Mn}^{\text{III}}$  atoms in a 1:2 ratio.

## Redox Properties

Cyclic voltammetry of **3** in water at neutral pH gives  $E_{1/2}$  values that correspond to the oxidation processes  $[\text{Mn}_2^{\text{III}}\text{Mn}^{\text{II}}] \rightarrow [\text{Mn}_3^{\text{III}}]$  at 0.106 V and  $[\text{Mn}_3^{\text{III}}] \rightarrow [\text{Mn}_2^{\text{III}}\text{Mn}^{\text{IV}}]$  at 0.395 V (Figure 3). We have intentionally chosen a neutral pH range for the present case in order to avoid the complications arising from POM-based redox processes.

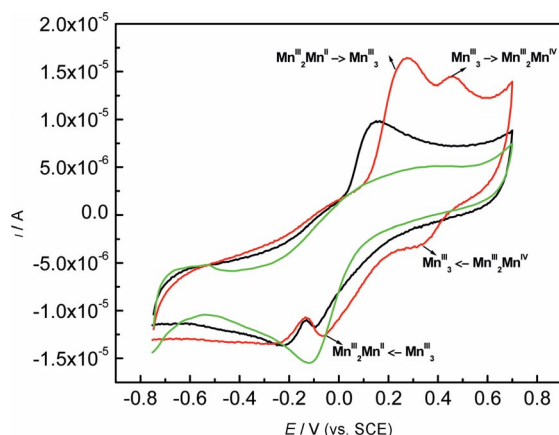


Figure 3. Comparison of cyclic voltammogram of (i) **3** in H<sub>2</sub>O with 0.10 M KCl used as supporting electrolyte (red line), (ii) **3** after deposition on the electrode surface during cyclic voltammetry studies in 0.10 M KCl (black line) and (iii) POM **2** in 0.10 M KCl (green line); scan rate = 50 mV s<sup>-1</sup>.

It is interesting to note that with an increase in the number of scans there is an increase in peak heights (Figure 4), which clearly indicates the progressive deposition of **3** on the electrode surface. Moreover, the deposited material gives a single oxidation peak ([Mn<sub>2</sub><sup>III</sup>Mn<sup>II</sup>] → [Mn<sub>3</sub><sup>III</sup>]) but not the [Mn<sub>3</sub><sup>III</sup>] → [Mn<sub>2</sub><sup>III</sup>Mn<sup>IV</sup>] transformation on the electrode surface (Figure 3). This result implies that this conversion occurs only in solution. The  $E_{1/2}$  value of the deposited material is cathodically shifted by 0.031 V ( $E_a = 0.152$  V and  $E_c = -0.091$  V), which means that the oxidized species (product) is more strongly adsorbed onto the electrode surface and thus inhibits the [Mn<sub>3</sub><sup>III</sup>] → [Mn<sub>2</sub><sup>III</sup>Mn<sup>IV</sup>] transformation because of its stability on the electrode surface. The parent POM **2** does not show any oxidation process under the identical experimental conditions. The peaks at -0.25 V (**3**), -0.22 V for the deposited materials on the electrode surface (**3**) and at -0.13 V for [SiW<sub>9</sub>O<sub>34</sub>]<sup>10-</sup> (**2**) are common and can be attributed to the reduction at the W<sup>VI</sup> centre in the POM fragments. It is interesting to note that, in the case of **3**, this peak is somewhat cathodically shifted both in solution and in the deposited phases.

The parallel analysis on the sample obtained from the controlled experiment by using Mn<sup>III</sup> acetate, Mn<sup>II</sup> acetate and **2** in a molar ratio 2:1:1 at the same sweep rate in aqueous solution (20 mL, 1.0 mmol dm<sup>-3</sup>) between -1.0 to +1.0 V shows two oxidation peaks at 0.46 and 0.66 V and a broad reduction peak at 0.35 V (vs. SCE). There is also no cathodical deposition of this material on the electrode surface (Figure 5) as indicated by the lack of any increase in peak current with an increase in the number of scans. We have also carried out the cyclic voltammetry studies on the precursor complex **1** in MeCN with tetrabutylammonium perchlorate as supporting electrolyte, and two reduction peaks appear at -0.25 and -1.08 V and the corresponding oxidation peaks appear at 1.16 and -0.41 V (vs. Ag/AgCl), respectively. Similar observations were also made in [Mn<sub>3</sub>(μ<sub>3</sub>-O)(μ-O<sub>2</sub>CCH<sub>2</sub>-1-NAPH)<sub>6</sub>(py)<sub>3</sub>] (HO<sub>2</sub>CCH<sub>2</sub>-1-NAPH = naphthylacetic acid).<sup>[15]</sup> It is therefore evident

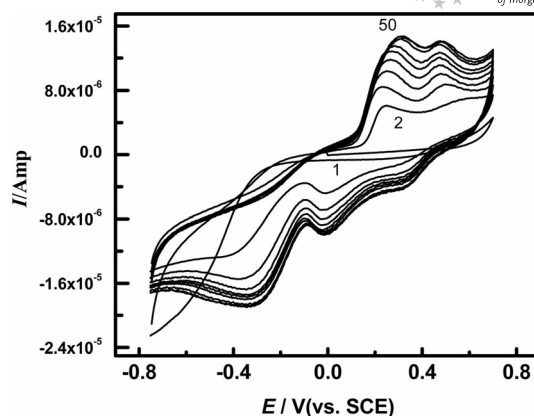


Figure 4. Cyclic voltammogram of **3** (1.0 × 10<sup>-3</sup> mol dm<sup>-3</sup>) in water with a sweep rate of 50 mV s<sup>-1</sup>.

from the perspective of the electrochemical studies that compound **3** is different from that prepared by mixing Mn<sup>III</sup> acetate, Mn<sup>II</sup> acetate and **2** in a 2:1:1 ratio.

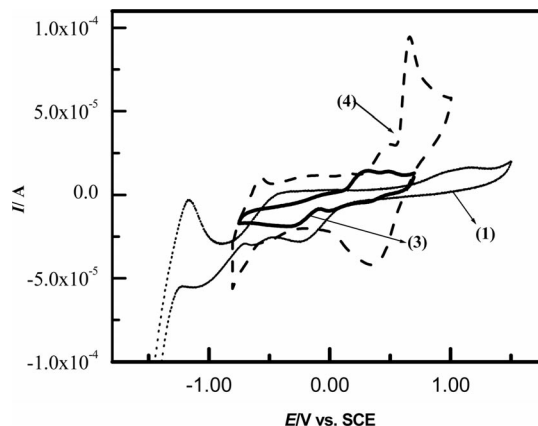


Figure 5. Cyclic voltammograms of 1.0 mmol dm<sup>-3</sup> of **3** and **4** in aqueous KCl (0.10 M) media and of **1** in MeCN (TBAP = 0.10 M). Sweep rate = 50 mV sec<sup>-1</sup>.

These experiments suggest that the mechanism of formation of **3** involves the direct insertion of the trinuclear, mixed-valence manganese precursor **1** into the three vacant sites of **2**, which subsequently displaces the carboxylate ligands by more basic oxo groups from the POM complex (Scheme 1). This assumption is strongly corroborated by the observations that (i) the reaction of trilacunary POM with precursors [Mn<sup>II</sup>Mn<sup>III</sup><sub>2</sub>(μ<sub>3</sub>-O)(X-benzoato)<sub>6</sub>(py)<sub>3</sub>] (X, 2-F, 2-Cl, 3-Cl) results in the same polyanion **3** and (ii) the reaction of Mn<sup>III</sup> acetate, Mn<sup>II</sup> acetate and **2** in the molar ratio 2:1:1 under the identical reaction conditions does not lead to **3** (the product obtained in this reaction is different from **3** as supported by cyclic voltammetry studies shown in Figures 3 and 5). Several attempts to generate single crystals for the latter reaction were not successful. The above hypothesis is further supported by the retention of the C<sub>3</sub> symmetry of the bridged [Mn<sub>3</sub>] unit as well as of the oxidation states [Mn<sup>II</sup>Mn<sup>III</sup><sub>2</sub>] even after its incorporation into the anion.



## Magnetic Properties

The magnetic susceptibility measurements reveal a paramagnetic behaviour of **3** in the temperature range 1.8–300 K (Figure 6). At room temperature, the  $\chi T$  product is about 10.1 cm<sup>3</sup> K/mol. Upon cooling, the  $\chi T$  product decreases very rapidly to reach a minimum value of about 4.0 cm<sup>3</sup> K/mol at 8.7 K before increasing, below 3 K, to reach 4.5 cm<sup>3</sup> K/mol at 1.8 K. This global behaviour reveals strong antiferromagnetic interactions between the Mn centres. By considering the molecular structure of the mixed-valence [Mn<sub>3</sub>] unit (inset, Figure 6), an isotropic Heisenberg triangular model with the following spin Hamiltonian was first used:

$$H = -2J(S_{\text{Mn}^{\text{III}}\text{A}} + S_{\text{Mn}^{\text{III}}\text{B}})S_{\text{Mn}^{\text{II}}} - 2J'S_{\text{Mn}^{\text{III}}\text{A}}S_{\text{Mn}^{\text{III}}\text{B}}$$

with  $S_i = 2$  and  $S_i = 5/2$  for the Mn<sup>III</sup> and Mn<sup>II</sup> metal ions, respectively, and  $J$  and  $J'$  are the exchange interactions in the trinuclear unit between adjacent Mn<sup>II</sup> and Mn<sup>III</sup> ions and between Mn<sup>III</sup> ions, respectively.

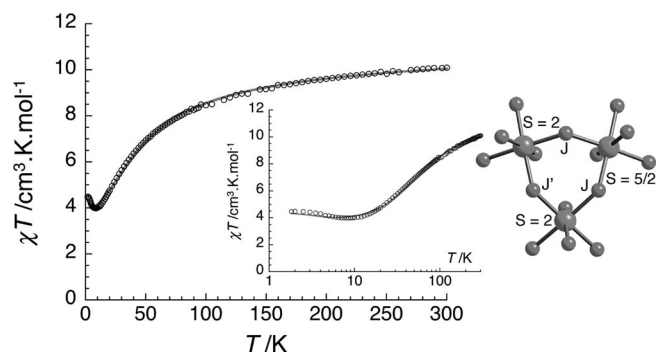


Figure 6.  $\chi T$  vs.  $T$  plot for **3** at 1000 Oe (where  $\chi$  is  $M/H$ ). The solid line is the best fit obtained with the Heisenberg trinuclear model described in the text. Inset:  $\chi T$  vs.  $T$  semi-log plot for **3** at 1000 Oe. A scheme of the spin topology is shown on the right side of the figure.

Application of the van Vleck equation<sup>[16]</sup> to the Kambe's vector coupling scheme<sup>[17]</sup> allows an analytical expression of the magnetic susceptibility as, for example, given by Vincent et al.<sup>[18]</sup> This Heisenberg model was able to reproduce the experimental data very well from 300 to 1.8 K as seen on Figure 6 with the best set of parameters:  $J/k_B = -1.3(1)$  K,  $J'/k_B = -7.8(1)$  K and  $g = 2.0(1)$ . The ground state of the [Mn<sub>3</sub>] unit is thus  $S = 5/2$  as further confirmed by the field dependence of the magnetization at 1.8 K (i.e. the magnetization is almost saturated at 7 T and reaches 5  $\mu_B$ ). As expected with regard to the dramatic change in the bridge natures between the Mn spin carriers in **3** relative to those in **2** (with carboxylate and  $\mu_3$ -O bridges), the magnetic interactions in the [Mn<sub>3</sub>] unit are completely modified even if they remain antiferromagnetic in nature and have a similar amplitude.<sup>[11]</sup> The most important change induced by the modification of the  $J/J'$  ratio is the spin ground state of the [Mn<sub>3</sub>] unit, which is 5/2 in **3**, while only 1/2 or 3/2 spin ground states are observed in the family of [Mn<sup>II</sup>-Mn<sup>III</sup>]<sub>2</sub>( $\mu_3$ -O)(X-benzoato)<sub>6</sub>(py)<sub>3</sub> precursors. Finally, it is

worth mentioning that the single-ion anisotropy of the Mn<sup>III</sup> sites have also been considered in a more sophisticated Heisenberg model,<sup>[19]</sup> but the quality of the simulation was not improved.

## Conclusions

In summary, a mixed-valence, manganese tricapped Keggin polyoxometalate has been designed by controlled insertion of three Mn atoms from [Mn<sup>II</sup>Mn<sup>III</sup>]<sub>2</sub>( $\mu_3$ -O)(2-Cl-benzoato)<sub>6</sub>(py)<sub>3</sub> into the vacant sites of the trilacunary precursor. Both [Mn<sub>3</sub>] and [A- $\alpha$ -SiW<sub>9</sub>O<sub>34</sub>]<sup>10-</sup> units have been assembled whilst keeping with a  $C_3$  symmetry and retain their original molecular structure. Magnetic measurements reveal that the final Mn<sub>3</sub>-POM complex possesses an antiferromagnetic coupling between Mn centres, which induces an  $S = 5/2$  ground state.

## Experimental Section

**Materials and Reagents:** Unless otherwise mentioned, materials (reagent grade) were obtained from commercial suppliers and used without further purification. The precursors [Mn<sub>3</sub>( $\mu_3$ -O)(2-Cl-benzoato)<sub>6</sub>(py)<sub>3</sub>] (**1**)<sup>[11]</sup> and Na<sub>10</sub>[A- $\alpha$ -SiW<sub>9</sub>O<sub>34</sub>]<sup>[20]</sup> (**2**) were prepared by using the literature procedures.

**Physical Methods:** Elemental analyses were carried out by using a Perkin–Elmer 240 elemental analyzer. IR spectra (400–4000 cm<sup>-1</sup>) were recorded in KBr pellets on a Nicolet Magna IR 750 series-II FTIR spectrophotometer. TGA/DTA thermograms were recorded on a Perkin–Elmer Pyris Diamond TGA/DTA thermal analyzer under a dynamic nitrogen environment. Electrochemical measurements were carried out by using a computer-controlled AUTOLAB (model 263A VERSASTAT) electrochemical system with glassy carbon as the working electrode, Pt-wire as the counter electrode and a saturated calomel electrode as the reference electrode. Cyclic voltammograms were recorded at 25 °C in deionized water from Millipore – Milli-Q Water Purification Systems under pure N<sub>2</sub> atmosphere with 0.1 M KCl as supporting electrolyte.

**Synthesis of {[Mn<sub>3</sub>(H<sub>2</sub>O)<sub>3</sub>SiW<sub>9</sub>O<sub>37</sub>]<sup>8-</sup>·24H<sub>2</sub>O(2Na<sup>+</sup>, 11K<sup>+</sup>, 3H<sup>+</sup>): [Mn<sub>3</sub>( $\mu_3$ -O)(2-Cl-benzoato)<sub>6</sub>(py)<sub>3</sub>] (**1**) (0.243 g, 0.18 mmol) in MeCN (15 mL), trilacunary Na<sub>10</sub>[A- $\alpha$ -SiW<sub>9</sub>O<sub>34</sub>] (**2**) (0.442 g, 0.18 mmol) and potassium chloride (0.16 g, 2.1 mmol) were treated in a simple one-pot reaction in aqueous acetic acid medium (pH = 4.50) in the molar ratio 1:1:11.6. Brown, hexagonal-shaped crystals of **3** suitable for X-ray analysis were obtained by slow evaporation at ambient temperature of the reaction solution (yield  $\approx$  30%). Elemental analysis: calcd. H 0.86; found 0.87%.**

**Magnetic Measurements:** The magnetic susceptibility measurements were obtained with the use of a Quantum Design SQUID magnetometer MPMS-XL housed at the Centre de Recherche Paul Pascal. This magnetometer operates between 1.8 and 300 K for dc applied fields ranging from -7 to 7 T. Measurements were performed on a polycrystalline sample of 26.87 mg. The magnetic data were corrected for the sample holder and diamagnetic contributions. Before any measurement, the samples were checked for the presence of ferromagnetic impurities by measuring the magnetization as a function of the field at 100 K. For pure paramagnetic or diamagnetic systems, a perfect straight line is expected and is observed for these compounds, which indicates the absence of any

ferromagnetic impurities; ac susceptibility measurements were measured with an oscillating ac field of 3 Oe and ac frequencies ranging from 1 to 1500 Hz, but it is worth noting that no out-of-phase ac signal (that could be the signature of single-molecule magnetic properties) was detected.

**X-ray Crystallography:** X-ray single-crystal diffraction measurements for complex **3** (Table 1) were carried out on a Bruker Smart 1000 CCD area detector diffractometer equipped with a graphite crystal monochromator. The determination of the unit-cell parameters and data collection were performed with Mo- $K_{\alpha}$  radiation ( $\lambda = 0.71073$  Å) by the  $\omega$ -scan mode. There was no evidence of crystal decay during data collection. The program SAINT<sup>[21]</sup> was used for integration of the diffraction profiles. Semiempirical absorption corrections were applied by using the SADABS program.<sup>[22]</sup> The structure was solved by a direct method by using the SHELXS program of the SHELXTL package and refined with SHELXL.<sup>[23]</sup> Metal atoms in complex **3** were located from the E-maps, and other non-hydrogen atoms were located in successive difference Fourier syntheses and refined with anisotropic thermal parameters on  $F^2$ . Some of the water hydrogen atoms were located from the difference Fourier map and refined isotropically.

Table 1. Crystallographic data for compound **3**.

Formula	(H <sub>6</sub> Mn <sub>3</sub> O <sub>40</sub> SiW <sub>9</sub> ) <sub>2</sub> · 24H <sub>2</sub> O(3H <sup>+</sup> , 11K <sup>+</sup> , 2Na <sup>+</sup> )
$F_w$	5871.31
Crystal System	trigonal
Space group	$R\bar{3}$ (no.148)
$a, b, c$ [Å]	12.4088(5), 12.4088(5), 52.0106(15)
$\alpha, \beta, \gamma$ [°]	90, 90, 120
$V$ [Å <sup>3</sup> ]	6935.6(4)
$Z$	3
$D_{\text{calcd.}}$ [g/cm <sup>3</sup> ]	4.217
$\mu(\text{Mo-}K_{\alpha})$ [mm]	23.736
$R(000)$	7827
Crystal size [mm]	0.08 × 0.11 × 0.14
$T$ [K]	273
$\lambda$ [Å]	0.71073
$\theta$ min, max [°]	1.2, 28.3
$h, k, l$	−16/16; −16/16; −69/69
Reflections: total, unique, $R(\text{int})$	19041, 3038, 0.052
Observed data [ $I > 2.0\sigma(I)$ ]	2480
$N_{\text{ref}}, N_{\text{par}}$	3038, 216
$R_1(F_o)$	0.0316
$wR_2(F_o)$ [ $I \geq 2\sigma(I)$ ]	0.0897
$S^a$	1.08

$$[a] S = \sum [w(F_o^2 - F_c^2)^2 / (n - p)]^{1/2}.$$

## Acknowledgments

M. A. thanks the University Grants Commission (UGC) for a research grant with potential for excellence under the UGC scheme of Jadavpur University, and the University Grants Commission (UGC) (Major), New Delhi and the Department of Science and Technology (DST), New Delhi for financial support. M. A. also thanks Prof. K. Das of Jadavpur University for helpful discussions. This work was also supported by MAGMANet (NMP3-CT-2005-515767), the University of Bordeaux (in particular for the visiting professorship of M. A.), the Centre National de la Recherche Scientifique (CNRS), the Region Aquitaine, the GIS Advanced Materials in Aquitaine (COMET Project) and the French Ministries of Foreign Affairs and Research.

- [1] Catalysis: examples of recent works include: a) M. Misono, *Chem. Commun.* **2001**, 1141–1152; b) A. M. Khenkin, L. Weiner, Y. Wang, R. Neumann, *J. Am. Chem. Soc.* **2001**, *123*, 8531–8542; c) I. V. Kozhevnikov, *Catalysts for Fine Chemicals, Catalysis by Polyoxometalates*, Vol. 2, Wiley, Chichester, U. K., **2002**; d) I. V. Kozhevnikov, *Innovations Pharm. Technol.* **2003**, *3*, 96–102; e) N. M. Okun, T. M. Anderson, K. I. Hardcastle, C. L. Hill, *Inorg. Chem.* **2003**, *42*, 6610–6612; f) I. Kiricsi, *Appl. Catal. A* **2003**, *256*, 1, special issue; g) C. L. Hill, *Angew. Chem. Int. Ed.* **2004**, *43*, 402–404; h) H. Liu, E. Iglesia, *J. Catal.* **2004**, *223*, 161–169; i) S. S. Stahl, *Angew. Chem. Int. Ed.* **2004**, *43*, 3400–3420.
- [2] Material Science: examples of recent works include: a) D. G. Kurth, P. Lehmann, D. Volmer, A. Müller, D. Schwahn, *J. Chem. Soc., Dalton Trans.* **2000**, 3989–3998; b) M. Clemente-León, E. Coronado, P. Delhaës, C. J. Gómez-García, C. Mingotaud, *Adv. Mater.* **2001**, *13*, 574–577; c) J. M. Clemente-Juan, E. Coronado, A. Forment-Aliaga, J. R. Galán-Mascarós, C. Giménez-Sáiz, C. J. Gómez-García, *Inorg. Chem.* **2004**, *43*, 2689–2694; d) A. Forment-Aliaga, E. Coronado, M. Feliz, A. Gaita-Ariño, R. Llusar, F. M. Romero, *Inorg. Chem.* **2003**, *42*, 8019–8027; e) N. Casañ-Pastor, P. Gómez-Romero, *Front. Biosci.* **2004**, *9*, 1759–1770; f) B. S. Bassil, S. Nellutla, U. Kortz, A. C. Stowe, J. van Tol, N. S. Dalal, B. Keita, L. Nadjio, *Inorg. Chem.* **2005**, *44*, 2659–2665; g) P. Mialane, A. Dolbecq, J. Marrot, E. Riviere, F. Sécheresse, *Chem. Eur. J.* **2005**, *11*, 1771–1778; h) M. A. AlDamen, J. M. Clemente-Juan, E. Coronado, C. Martí-Gastaldo, A. Gaita-Ariño, *J. Am. Chem. Soc.* **2008**, *130*, 8874–8875; i) C. Ritchie, A. Ferguson, H. Nojiri, H. N. Miras, Y.-F. Song, D.-L. Long, E. Burkholder, M. Murrie, P. Kögerler, E. K. Brechin, L. Cronin, *Angew. Chem.* **2008**, *47*, 5609–5612; j) J.-D. Compain, P. Mialane, A. Dolbecq, I. M. Mbomekallé, J. Marrot, F. Sécheresse, E. Riviere, G. Rogez, W. Wernsdorfer, *Angew. Chem.* **2009**, *48*, 3077–3081.
- [3] Medicine: examples of recent works: a) I. M. Botto, D. A. Barrio, M. G. Egusquiza, C. I. Cabello, A. M. Cortizo, S. B. Etcheverry, *Met. Ions Biol. Med.* **2002**, *7*, 159; b) X. Wang, J. Liu, J. Li, Y. Yang, J. Liu, B. Li, M. T. Pope, *J. Inorg. Biochem.* **2003**, *94*, 279–284; c) X. Wang, J. Liu, M. T. Pope, *Dalton Trans.* **2003**, 957–960.
- [4] Photochemistry: examples of recent works: a) T. Yamase, P. V. Prokop, *Angew. Chem. Int. Ed.* **2002**, *41*, 466–469; b) T. Ruether, V. M. Hultgren, B. P. Timko, A. M. Bond, W. R. Jackson, A. G. Wedd, *J. Am. Chem. Soc.* **2003**, *125*, 10133–10143.
- [5] a) L. C. W. Baker, V. E. S. Baker, K. Eriks, M. T. Pope, M. Shibata, O. W. Rollins, J. H. Fang, L. L. Koh, *J. Am. Chem. Soc.* **1966**, *88*, 2329–2331; b) L. C. W. Baker, J. S. Figgis, *J. Am. Chem. Soc.* **1970**, *92*, 3794–3797.
- [6] a) U. Kortz, Y. P. Jeannin, A. Tézé, G. Hervé, S. Isber, *Inorg. Chem.* **1999**, *38*, 3670–3675; b) U. Kortz, S. Matta, *Inorg. Chem.* **2001**, *40*, 815; c) F. Hussain, B. S. Bassil, L.-H. Bi, M. Reicke, U. Kortz, *Angew. Chem. Int. Ed.* **2004**, *43*, 3485–3488; d) B. S. Bassil, S. Nellutla, U. Kortz, A. C. Stowe, J. van Tol, N. S. Dalal, B. Keita, L. Nadjio, *Inorg. Chem.* **2005**, *44*, 2659–2665.
- [7] a) K.-C. Kim, A. Gaunt, M. T. Pope, *J. Cluster Sci.* **2002**, *13*, 423–436; b) J. Canny A. Teze, R. Thouvenot, G. Herve, *Inorg. Chem.* **1986**, *25*, 2114–2119.
- [8] a) L.-H. Bi, U. Kortz, *Inorg. Chem.* **2004**, *43*, 7961–7962; b) U. Kortz, N. K. Al-Kassem, M. G. Savelieff, N. A. Al Kadi, M. Sadakane, *Inorg. Chem.* **2001**, *40*, 4742–4749; c) T. J. R. Weakley, R. G. Finke, *Inorg. Chem.* **1990**, *29*, 1235–1241; d) L.-H. Bi, R.-D. Huang, J. Peng, E.-B. Wang, Y. H. Wang, C.-W. Hu, *J. Chem. Soc., Dalton Trans.* **2001**, 121–129; e) U. Kortz, S. Isber, M. H. Dickman, D. Ravot, *Inorg. Chem.* **2000**, *39*, 2915–2922.
- [9] J. Liu, F. Ortega, P. Sethuraman, D. E. Katsoulis, C. E. Costello, M. T. Pope, *J. Chem. Soc., Dalton Trans.* **1992**, 1901–1906.

- [10] a) O. Kahn, *Molecular Magnetism*, VCH: New York, **1993**; b) R. L. Carlin, *Magnetochemistry*, Springer-Verlag: Berlin, **1986**.
- [11] J. Ribas, B. Albela, H. Stoeckli-Evans, G. Christou, *Inorg. Chem.* **1997**, *36*, 2352–2360.
- [12] X. Fang, P. Kögerler, *Chem. Commun.* **2008**, 3396–3398.
- [13] D. Altermatt, I. D. Brown, *Acta Crystallogr., Sect. B* **1985**, *41*, 240–244.
- [14] X.-Y. Zhang, C. J. O'Connor, G. B. Jameson, M. T. Pope, *Inorg. Chem.* **1996**, *35*, 30–34.
- [15] S. Yano, M. Nakai, H. Ohi, T. Funabiki, R. Tanaka, I. Kinoshita and M. Obata, Ed. J. F. Allen, E. Gantt, J. H. Golbeck and B. Osmond, *Photosynthesis: Energy from the Sun, 14th International Congress on Photosynthesis*, Glasgow, **2007**.
- [16] J. H. van Vleck, *The Theory of Electric and Magnetic Susceptibility*, Oxford University Press, **1932**.
- [17] K. Kambe, *J. Phys. Soc. Jpn.* **1950**, *5*, 48–51.
- [18] J. B. Vincent, H. R. Chang, K. Folting, J. C. Huffman, G. Christou, D. N. Hendrickson, *J. Am. Chem. Soc.* **1987**, *109*, 5703–5711.
- [19] a) J. J. Borrás-Almenar, J. M. Clemente-Juan, E. Coronado, B. S. Tsukerblat, *Inorg. Chem.* **1999**, *38*, 6081; b) J. J. Borrás-Almenar, J. M. Clemente-Juan, E. Coronado, B. S. Tsukerblat, *J. Comput. Chem.* **2001**, *22*, 985.
- [20] G. Herve, A. Teze, *Inorg. Chem.* **1992**, *31*, 4128–4133.
- [21] AXS Bruker, *SAINT Software Reference Manual*, Madison, WI, **1998**.
- [22] G. M. Sheldrick, *SADABS, Siemens Area Detector Absorption Corrected Software*, University of Göttingen, Germany, **1996**.
- [23] G. M. Sheldrick *SHELXTL NT, Version 5.1, Program for Solution and Refinement of Crystal Structures*, University of Göttingen, Germany, **1997**.

Received: May 31, 2010

Published Online: November 5, 2010